

Attitude Control on GRACE Follow-On: Experiences from the First Years in Orbit



F. Cossavella, J. Herman, L. Hoffmann, D. Fischer, H. Save, B. Schlepp, and T. Usbeck

Abstract The two satellites for the GRACE (Gravity Recovery And Climate Experiment) Follow-On mission were successfully launched in May 2018 into a polar orbit at an altitude of 491 km. Its predecessor GRACE was operated by the same partners from 2002 until 2017). The mission continues the measurements of the gravity field of the Earth (with emphasis on the time variability) and also delivers radio occultation measurements. The twin satellites are kept at a relative distance of 170 to 270 km and act as probes in the gravity field of the Earth. The inter-satellite distance is measured by a microwave tracking system to an accuracy of 1 μm . A laser ranging interferometer is added as a technology demonstration. Stable and accurate relative pointing, as well as the minimization of disturbance torques, is required in order to optimize scientific results. This poses stringent demands upon attitude control. The performance of the GRACE Follow-on attitude control system will be presented, as well as the special actions and changes that became necessary as the mission evolved. A short description of the sensors and actuators used for attitude control is given and improvements with respect to GRACE are discussed in some more detail. The operational modes are described with a focus on the so-called nominal fine-pointing mode, in which the front ends point towards each other in order to enable microwave- and

F. Cossavella (✉) · J. Herman · L. Hoffmann · B. Schlepp
Deutsches Zentrum Für Luft-und Raumfahrt e.V. (DLR), Oberpfaffenhofen, Germany
e-mail: Fabiana.Cossavella@dlr.de

L. Hoffmann
e-mail: L.Hoffmann@dlr.de

B. Schlepp
e-mail: Benjamin.Schlepp@dlr.de

D. Fischer · T. Usbeck
Airbus Defence and Space - Space Systems, Immenstaad, Germany
e-mail: Denis.Fischer@airbus.com

T. Usbeck
e-mail: Thomas.Usbeck@airbus.com

H. Save
Center for Space Research, The University of Texas, Austin, TX, USA
e-mail: save@csr.utexas.edu

laser-ranging. The third section opens with a description of special tasks, such as the fine-tuning of the control and monitoring parameters and the complex determination of the satellite's center of gravity. A comparison is made with a tracking model based upon the fuel expenditure from the two tanks that can be determined independently. Several series of involved tests with manual thruster firings were performed in order to characterize the response of the accelerometers to thruster actuations. A description of the design of the tests, their execution and results is presented. A switch to the redundant instrument was made five months after launch on one of the satellites. The consequences for attitude control are discussed in Sect. 4. A method that was developed to cope with a situation where also the redundant GPS receiver would become unavailable is discussed in detail. Conclusions and an outlook for the upcoming years of operations are presented in the last section.

Keywords GRACE-FO · AOCS

Acronyms/Abbreviations

ASM	Acquisition and Safe mode
ASM-RD	ASM Rate Damping
ASM-CP	ASM Coarse Pointing
ASM-SS	ASM Steady State
AOCS	Attitude and Orbit Control System
ACT	Attitude Control Thruster
CESS	Coarse Earth and Sun Sensor
CGPS	Cold Gas Propulsion System
CoM	Center of Mass
CMC	Center of Mass Calibration
DLR	Deutsches Zentrum für Luft- und Raumfahrt–German Aerospace Center
FDIR	Failure Detection, Isolation and Recovery
FDS	Flight Dynamic System
FGM	Fluxgate Magnetometers
GFZ	GeoForschungsZentrum–German Research Center for Geosciences
GPS	Global Positioning System
GRACE	Gravity Recovery And Climate Experiment
GRACE-FO	Grace Follow-on
GF1	Grace Follow-on 1
GF2	Grace Follow-on 2
GSOC	German Space Operations Center
IMU	Inertial Measurement Unit
IPU	Instrument Processing Unit
JPL	Jet Propulsion Laboratory
LEOP	Launch and Early Orbit Phase

LRI	Laser Ranging Interferometer
MTQ	Magnetic Torquers
NOM	Normal Mode
OBC	On-Board Computer
OCM	Orbit Control Mode
OCT	Orbit Control Thruster
OD	Orbit Determination
OOP	On-board Orbit Propagator
PVT	Pressure-Volume-Temperature
RTN	Radial Tangential Normal
STR	Start Tracker
STR1	Start Tracker head 1
STR2	Start Tracker head 2
STR3	Start Tracker head 3
STRE	Start Tracker Electronics
TLEs	Two-Line Elements

1 Introduction

GRACE Follow-On is a scientific co-operation between the USA and Germany, following the model initiated by its predecessor GRACE [1, 2]. The twin satellites were built by Airbus Defence and Space in Germany, under a contract from NASA's Jet Propulsion Laboratory (JPL). Operations are carried-out at the German Space Operations Center (DLR-GSOC) on behalf of the German Research Center for Geosciences (GFZ).

The main scientific goal of the mission is to collect data for creating both static and time-varying maps of the terrestrial gravity field. The satellites were launched in May 2018 at an altitude of 491 km on a circular polar orbit. They are kept at a relative distance of 170 to 270 km and act as probes in the gravity field of the Earth. The inter-satellite distance is measured by a microwave tracking system to an accuracy of 1 μm ; a laser ranging instrument (LRI) is added as a technology demonstration and has improved the accuracy of the distance measurements by a factor of 30 [3, 4]. Non-gravitational disturbances can be determined with a SuperStar accelerometer.

The front-ends of the satellites have to point towards each other to enable microwave- and laser-ranging. Stable and accurate relative pointing and the minimization of disturbance torques are required in order to optimize scientific results. This poses stringent demands upon attitude control.

A short description of the sensors and actuators of the attitude and orbit control system (AOCS) is given in the next section. Improvements with respect to GRACE are discussed in some more detail, in particular those for the star cameras and the inertial measurement units.

The performance of the AOCS during nominal operation is evaluated based on the data collected during the first two and a half years in orbit. A description of several special activities necessary to improve the analysis of the scientific data is given with particular emphasis on the consequences for the attitude control of the satellite.

A switch to the redundant instrument was made five months after launch on one of the satellites [5]. This comprised not only a switch of the instrument processing unit, but also of the ultra-stable oscillator, GPS receiver, microwave assembly and electronics. The consequences for attitude control are discussed in the Sect. 4, together with a modified operational approach to bridge several months without on-board GPS data.

2 The Attitude and Orbit Control System

The design of the GRACE-FO satellites benefits from the experience gained from their predecessors. In particular the number and quality of the sensors has been improved [6]. A schematic view of one of the satellites is shown in Fig. 1, a detailed description of the satellite layout can be found in [2].

The Coarse Earth and Sun Sensors (CESS) provides attitude measurements with respect to the direction of Sun and Earth. It consists of six sensor heads allocated along each axis, pair wise in opposite directions, in order to provide a spherical field of view. Each head consists of six thermistors, three for the detection of infrared light and three for the detection of Sun light, providing a 2-out-of-3 redundancy.

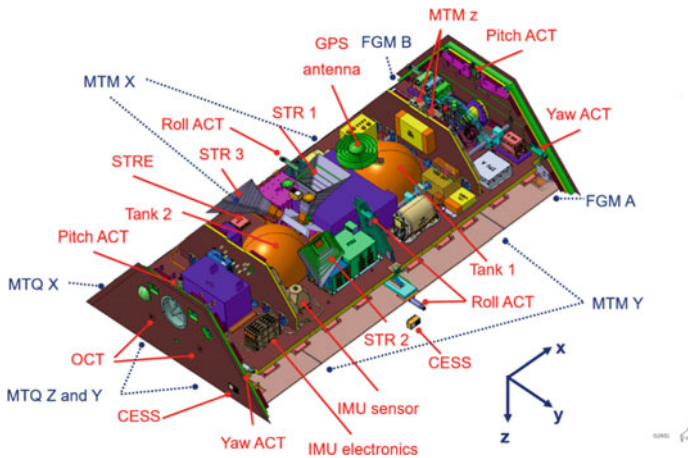


Fig. 1 Layout of one of the satellites (solar panels not shown). The location of the visible AOCS units is shown by red arrows. The dashed blue lines indicate the approximate location of units that are hidden

The magnetic field is measured by one of two fluxgate magnetometers (operated in cold redundancy) with an accuracy of ~ 300 nT. Each magnetometer consists of three independent magnetic sensors aligned to the satellite axes and operating simultaneously. The measurements are input for control with the magnetic torque rods and are also used as back-up computation of the rotation rates in acquisition and safe mode.

The use of a high-performance Inertial Measurement Unit (IMU) with four independent axes provides accurate rate measurements. A tetrahedral configuration of the inertial sensors offers one-failure tolerance. Three sensors are used during nominal operations, the fourth only after a transition into safe mode. On GRACE a medium performance IMU with three measurement axes was available, providing no redundancy.

GRACE had two star cameras of which only one was actively used for AOCS. GRACE-FO has three star-tracker heads with a separation between their boresights of 80.4° to 100° . The three STRs are used in hot redundancy and are connected to one of two electronic units which are operated in cold redundancy. The data are handled by the on-board computer (OBC) directly, whereas on GRACE they were collected and processed by the instrument processing unit before being handed to the OBC for use by the AOCS. This configuration optimizes the coverage and increases the accuracy of the attitude measurement in all three satellite axes. The new generation of star cameras can handle partial Moon intrusions and the on-board software autonomously delivers fused attitude data from one, two or three cameras depending upon validity.

As on GRACE, GPS data are provided by a dual-band receiver and the data are handled by the processing unit of the microwave instrument (IPU). These data are used to initialize the on-board orbit propagator (OOP) at each AOCS cycle.

The attitude is controlled primarily by a set of cold redundant magnetic torque rods (MTQs) of 27.5 Am^2 each. Each rod has a double coil providing cold redundancy. The rods are aligned with the axes of the satellite and located at maximum distance from the magnetometers in order to minimize disturbances on the magnetic field measurements. The MTQs are supplemented by a cold gas propulsion system with a set of twelve 10 mN attitude control thrusters (ACTs), separated into two branches. Two gas tanks of equal volume are mounted symmetrically along the x-axis of the spacecraft and are connected each to one of the branches, which are operated simultaneously to ensure an even depletion of the tanks. The design is inherited from GRACE with state-of-the-art enhancements and small improvements such as a two-stage pressure regulator that assures a constant feed pressure for the thrusters over the whole range of tank pressures. Two orbit control thrusters of 50 mN thrust, located at the rear part of the satellite, complete the cold gas propulsion system.

2.1 Attitude Modes and Frames of Reference

There are three main AOCS operation modes. The Acquisition and Safe Mode (ASM) is designed to guarantee power and thermal survival of the spacecraft, the Normal Mode (NOM) is the normal operating mode providing accurate three-axis attitude control according to the defined reference, and the Orbit Control Mode (OCM) is used for the necessary orbit change and maintenance maneuvers during the mission.

In addition, a reference attitude can be independently set by defining a frame of reference and a pointing bias. The pointing bias can be defined for each axis as Euler angle and it is added to the target attitude defined by the frame of reference.

The available frames of reference are the Nadir Pointing Frame, the Relative Pointing Frame and the Orbit Control Frame. In Nadir Pointing the z-axis of the satellite is aligned to the nadir direction, the y-axis is perpendicular to the plane defined by the z-axis and the velocity vector, and the x-axis is roughly pointed in the flight direction. The Orbit Control frame aligns the x-axis with the spacecraft velocity vector, the y-axis is perpendicular to the orbit plane and in the direction of the orbit normal vector. The z-axis completes the right-handed system.

As the horn antenna of the microwave instrument is located at the front of the satellite, in order to establish a link the two GRACE-FO spacecraft must point towards each other. When the Nadir frame is selected, a 180° yaw bias must be applied to rotate the leading satellite towards the trailing one. Precise inter-satellite pointing, however, is ensured only by selecting the Relative Pointing frame. This points the +x-axis to the other satellite, following a trajectory generated by an on-board algorithm according to an inter-satellite line of sight reference with the z-axis pointing towards Earth. The mutual distance is kept at 220 ± 50 km, which leads to a continuous small pitch bias of roughly -1° . The slowly varying mutual distance implies that the desired attitude is not a constant. The continuous knowledge of the position of the satellite and its partner is essential for the determination of the Relative Pointing frame. Therefore, each day the latest result of the orbit determination for both satellites are up-loaded to both satellites in form of Two-Line-Elements (TLEs). See also Sect. 4.3.

Attitude biases around the pitch and roll axes are nominally not commanded and used only during the calibration of the K-Band antenna pattern.

2.1.1 Acquisition and Safe Mode

ASM is autonomously entered after a mode drop by FDIR from the higher attitude modes, or after an on-board computer boot. The mode is divided into three sub-modes: rate damping (RD), coarse pointing (CP) and steady state (SS).

The ASM-RD is the point of entry of the ASM, the main task is to reduce the satellite rates to less than $0.2^\circ/\text{s}$, no control of the attitude is performed. The spacecraft rotation rate is measured by the IMU or derived from CESS and magnetometer measurements in case of non-availability of IMU data.

In ASM-CP a coarse nominal pointing of the satellite is achieved, with the z-axis of the satellite directed towards Earth and a yaw angle of 0° or 180° , depending on which value is closer to the current attitude.

The ASM-SS keeps the spacecraft in a coarse Earth-pointing attitude. The more powerful battery on GRACE-FO (78Ah name-plate capacity on GRACE-FO compared to 18Ah on GRACE) tolerates temporary yaw deviations of up to 60° in safe mode. No “yaw-steering” concept [7], forcing one of the side panels towards the Sun, is applied on GRACE-FO in ASM-SS.

The ASM mode intrinsically uses the Nadir Pointing frame as reference.

2.1.2 Normal Mode

NOM is the normal operating mode and it provides accurate Earth-pointing attitude according to the defined reference. The reference attitude is derived from the spacecraft position and velocity state vector provided by the GPS or, in case of a GPS outage, by an AOCS on-board orbit propagator.

The normal mode is subdivided into an intermediate acquisition sub-mode (ACQ), the Attitude Hold (AH) and the Fine Pointing (FP) sub-modes.

The NOM-ACQ is the entry point of the normal mode from coarse pointing in ASM or from OCM. The spacecraft acquires a specified 3-axis attitude relative to the selected frame, with an accuracy better than 30 mrad at 3σ confidence level. Rotations of the spacecraft of 180° in yaw are always performed in this mode.

Attitude Hold is entered from NOM-ACQ or from the NOM-FP and it holds the reference 3-axis attitude, with an absolute pointing error (at 3σ confidence level) better than 10 mrad in roll, and better than 5 and 3 mrad in yaw and pitch respectively. The attitude hold mode is used for center of mass calibrations and any other special AOCS operation that could lead to not nominal attitude disturbances, as for example an update of the NOM-FP controller settings or specific thruster tests.

The NOM-FP is the mode that provides high accuracy attitude pointing for science operation. The roll axis is controlled with an accuracy better than 2 mrad, whereas the pitch and yaw axes are controlled with an accuracy better than 0.25 mrad at 3σ confidence level. A science configuration is established once the Relative Pointing is activated in NOM-FP.

The use of TLEs to point towards the partner satellite is on GRACE-FO not restricted to the fine pointing (science) mode. This can be set by command in any NOM sub-mode, thus allowing for extra flexibility when performing special tests.

In all NOM sub-modes, the inertial attitude information is derived from accurate autonomous star sensor measurements and propagated to the current on-board time using measurements of the spacecraft rate from the high accuracy IMU. Attitude measurements from at least two star sensors are fused together, in order to achieve low noise in all axes by eliminating the star sensor boresight noise, which is typically 10 times higher than the cross-axis noise.

The spacecraft rate is also derived from star sensor measurements, as back-up in case of non-availability of IMU data. The CESS is used for FDIR surveillance of Sun/Earth angles in the normal mode.

Actuation is performed mainly by the magnetic torquers, augmented by the cold gas thrusters whenever necessary. The thrusters are operated with different sets of thrust limitation parameters according to the actual state of the attitude and rate errors. Magnetorquer control is based on on-board magnetometer measurements. The NOM-AH mode reflects the GRACE Attitude Hold Mode except for orbit control maneuvers and the NOM-FP mode the GRACE Science Mode [7].

2.1.3 Orbit Control Mode

This mode is used for the necessary orbit change and maintenance maneuvers during the mission under direct ground control. It provides the same principal functionality as the NOM-AH mode and uses the same equipment plus the orbit control thrusters, which are disabled in NOM. The OCM has no sub-modes.

2.2 AOCS Performance

The AOCS on GRACE-FO has shown a very stable behavior since launch. Both satellites have been commanded to NOM-FP ~21 h after separation; GF1 and GF2 have since then maintained fine pointing for more than 98% and 93% of the time, respectively.

The science configuration, i.e. simultaneous NOM-FP and Relative Pointing on both satellites, has been maintained for 86% of the mission life time. It was interrupted by maintenance phases to execute specific AOCS activities or orbit maneuvers, and by AOCS safe modes.

In order to maintain the twin satellites within a relative distance of 220 ± 50 km, five orbit control maneuvers were executed on GF1 and six on GF2 (of which one, however, was a collision avoidance maneuver made in 2018).

The longest interruptions of the science configuration were two prolonged periods in ASM and NOM-Nadir- Pointing on GF2, caused by an outage of the prime instrument processing unit in 2018 that left the AOCS without GPS data for a few months (see Sect. 4) and by an OBC switch to the back-up unit in early 2019 [8]. GF2 has spent a total of ~32 days in ASM, GF1 less than 5. Fuel consumption on GRACE-FO is considerably smaller than it was for GRACE, although the pointing performance is considerably better [3, 6]. In ASM an average gas consumption of 2.5 g/day and 5 g/day has been observed on GF1 and GF2 respectively, smaller than the initially allocated budget of 30 g/day and with some variations according to the angle of the Sun with respect to the orbital plane. This is a factor of 20 to 100 less as compared to GRACE. The nominal modes perform also better on GRACE-FO than on GRACE, with an average expenditure for both satellites of about 0.7 g/day in fine pointing

mode (cf. 3–5 g/d in the equivalent Science Mode on GRACE) and ~1 g/day in attitude hold mode (cf. 10 g/d in Attitude Hold Mode on GRACE).

The GRACE-FO satellites were launched with ~32 kg nitrogen gas and have consumed in the first 2.5 years of life about 1.2 kg of fuel. Such a low fuel consumption would allow to operate the satellites for another 60 years, although without an active altitude maintenance they will re-enter in the Earth atmosphere much earlier. The extra fuel can therefore be used to manage the altitude to increase the lifetime and improve the science products.

2.2.1 Fuel Consumption

Two methods are used to track the accumulated gas expenditure: the book-keeping method and the Pressure-Volume-Temperature (PVT) method.

The book-keeping is based on precise tracking of the total amount of time each thruster has been activated, and on knowledge of the thruster feed pressure and mass flow rate of each thruster unit. The mass flow rates at a reference feed pressure of 1.5 bar are known from calibrations of thrusters done on ground and the thruster on-times are recorded on board with one millisecond precision. The feed pressure in each propulsion branch is also available in the spacecraft telemetry. As the mass flow rates scale linearly with the feed pressure, it is possible to track how much gas has been ejected by each thruster over time.

The PVT method uses a combination of on-board and ground information together with the equation of state for a real gas to estimate the amount of mass in each pressure vessel:

$$m = \frac{P \cdot V}{R \cdot T \cdot Z}$$

where P is the pressure of the tank, V its volume, T its temperature, R is the universal gas constant and Z is the compressibility factor. Temperature and pressure of each tank are available in the on-board telemetry, whereas the volume of the vessel has been measured on ground before launch. In this work, a modified van der Waals approach to estimate the compressibility factor is used. The accuracy in the measurement of the gas temperature and pressure is the main source of uncertainty in this method, which can estimate the propellant mass with an accuracy of a few percent. Because the temperature sensors are located on the outer surface of the vessels, the PVT method does not provide accurate results during phases of fast cooling and heating of the nitrogen gas.

The book-keeping method is more suitable for calculating the consumption of the propellant mass but it is less sensitive to small leakages in the system. A comparison between the two methods is used as an indicator for leaks in the propulsion system. In Fig. 2 the estimated propellant expenditure for both tanks on each satellite is shown. Estimates with the book-keeping method show on both satellites a slightly higher consumption of gas from tank 2 (located along the minus x-axis) because of

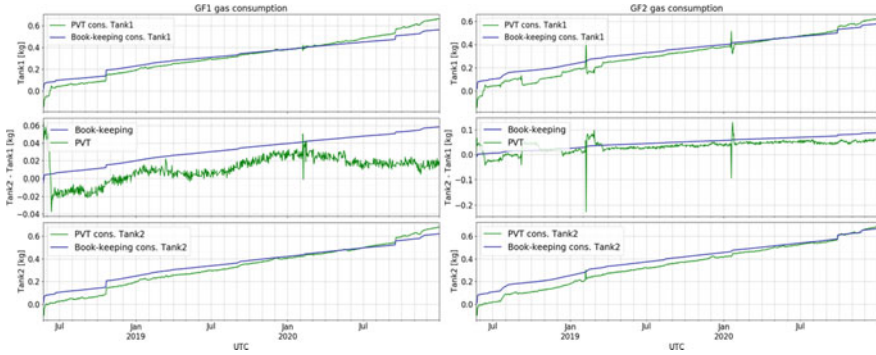


Fig. 2 Expenditure of gas on GF1 (left panel) and GF2 (right panel) as estimated with the PVT and book-keeping methods. The consumption of gas from tank 1 and tank 2 is displayed on the top and bottom panels, respectively. In the middle panel the difference in gas consumption between the two tanks is shown. Both satellites have consumed about 1.2 kg of nitrogen gas, with 25 to 60 g more gas taken from tank 2. Spikes in the used mass estimated from the PVT method coincide with fast cooling phases that followed the switch-off of both science instruments. This happened on GF2 in early 2019 and early 2020, and on GF1 in early 2020. The effect is stronger on tank 1, because it is closer to the instruments that are located near the front side of the satellite

the higher average feed pressure measured on the corresponding branch. The trend is confirmed by the results of the PVT mass estimation for all tanks, within the method uncertainties. On GF1, however, a small divergence between the results of two methods has been observed in the second half of 2020 and it is currently being investigated.

2.2.2 Star Tracker Performance

The boresight of STR1 is close to the $-z$ -axis of the satellite, whereas the boresight of STR2 and STR3 is close to the $+y$ and $-y$ -axis respectively (see Fig. 1). The use of three instead of two camera heads (as on GRACE) improves the availability and accuracy of attitude data about all spacecraft axes. Fused data from all three heads were delivered for approximately 70% of the time in the first two and a half years of the mission, whereas 0.2% of the time attitude data were derived from a single head only (the other two being blinded by the Sun and the Moon simultaneously; see Table 1). The individual heads deliver valid data for 87–94% of the time.

The performance of GF1 STR2 has to be compared to that of STR3 on GF2, because GF1 flies backwards with a 180° yaw bias with respect to the Nadir frame. The same applies for GF1 STR3 and GF2 STR2.

The precession of the orbital plane has an inertial period of about 320 days (β' cycle), implying that for ~ 160 days the Sun is on one side and for ~ 160 days on the other side of the satellite. β' denotes the angle between the orbital plane and the direction to the Sun.

Table 1 Percentage of quaternion samples derived from the fusion of the data from 3, 2 or 1 star tracker heads (upper half) and percentage of valid samples delivered by each star tracker head (lower half) with respect to the unit on-time, after 2.5 years in orbit

	% of on-time	
	GF1	GF2
<i>Fusion type</i>		
3 star cameras	71.06	69.94
2 star cameras	28.77	29.19
1 star camera	0.17	0.17
<i>Validity</i>		
STR 1	93.95	93.28
STR 2	87.70	86.86
STR 3	89.17	88.25

The behavior of each head depends on the phase in the β' cycle. STR1 is blinded by Sun for β' around 0° (phase = 0.0 and 0.5), GF1 STR3 and GF2 STR2 are blinded by Sun for β' around -90° (phase = 0.75), while for GF1 STR2 and GF2 STR3 this happens as β' approaches $+90^\circ$ (phase = 0.25) (see Fig. 3).

The slightly lower performance of GF2 STR2, as compared to GF1 STR3, is due to an anomalous behavior of the star tracker head in January 2019, when 90% of the measurements were invalid. Although the satellites were going for the first time through a β' minimum, the same behavior was not observed on GF1 STR3. The anomaly was most likely caused by condensation on the lens of the star tracker 2

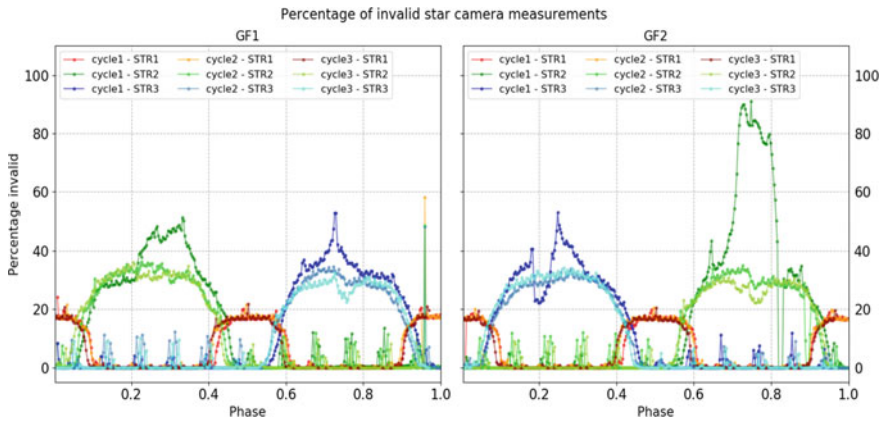


Fig. 3 Percentage per day of invalid measurements of the several star tracker heads as a function of the phase in the β' cycle. The performance of the STR for GF1 and GF2 is displayed in the left and right panels, respectively. The small peaks of 10% occurring every month on both satellites are due to intrusion of the Moon in the field of view of the star cameras. The high number of invalid STR2 samples during cycle one on GF2, starting at phase = 0.7, was probably caused by a condensation on the lens of the camera. The period with low percentages around phase = 0.2 on GF2 during cycle one is due to a prolonged period in ASM (fewer and shorter blindings due to the larger yaw deviations allowed)

head. This hypothesis is confirmed by the nominal behavior of the star tracker head, when the same phase of the β' cycle was reached in the following cycles (see Fig. 3).

The alignment of each star camera head to the spacecraft frame of reference was determined on ground before launch [2]. Once in orbit, the relative alignment between the STR heads has been measured from the attitude data. The zenith star camera was chosen as a reference. For the side STR sensors, the angle between the in-flight and on-ground calibrated mounting quaternions has been found to be between 0.4 and 0.6 mrad for each analysed quaternion pair. Attitude disturbances have been observed on both satellites when a STR head is excluded from the fusion process, usually because blinded by Sun or Moon. The effect is best visible when two out of three heads are simultaneously excluded and only one of the side cameras remains available. Attitude errors of about 0.5 mrad and occasionally up to 1 mrad were observed on the pitch axis in such cases, whereas nominally the pitch axis is controlled to better than 0.3 mrad. Although this level of disturbance is completely within the control capability of the NOM-FP mode, it led to a higher number of MTQ and pitch thruster actuations and could potentially disturb the science measurements.

The alignments for STR2 and 3 were updated in June 2020 to ensure a smoother transition if control is switched from one configuration to another. The analysis of the attitude errors after the star camera alignments were updated indicates that the existing bias has been significantly reduced, although there is an intrinsic lower accuracy when only one camera head is used. Almost two years of data have been analysed, starting in March 2019. The data set has been divided into 5 sub-sets based on the number of star camera heads available for attitude determination. For each sub-set, the average attitude error along each axis was calculated before and after the update of the star tracker alignments. Only days with nominal attitude and no special AOCs activities have been selected, resulting in a total of roughly 430 days before and 255 days after the update. The result for the pitch axis is shown in Fig. 4. The corresponding mean and standard deviation are reported in Table 2. On GF1 the average pitch error before the update of the alignments was -0.29 mrad when only measurements from STR2 were available, and 0.12 mrad when only measurements from STR3 were available. In contrast, the average attitude error was -0.05 mrad when all cameras were available. After the update, the average changed to 0.02 mrad and -0.10 mrad for the case in which only STR2 and only STR3 were valid, respectively. The standard deviation of the errors did not improve because this is not due to a misalignment but rather due to the lower accuracy of the measurements made with only one head. Similar results have been observed for GF2.

The number of daily actuations of the pitch thrusters has also been reduced after the update of the alignments and on GF1 no day with more than 30 actuations has been observed anymore. The results are summarized in Table 3 for both satellites and are consistent with the observations from the analysis of the attitude errors.

An improvement was also observed for the roll and yaw axes, but it is less significant and therefore not discussed here.

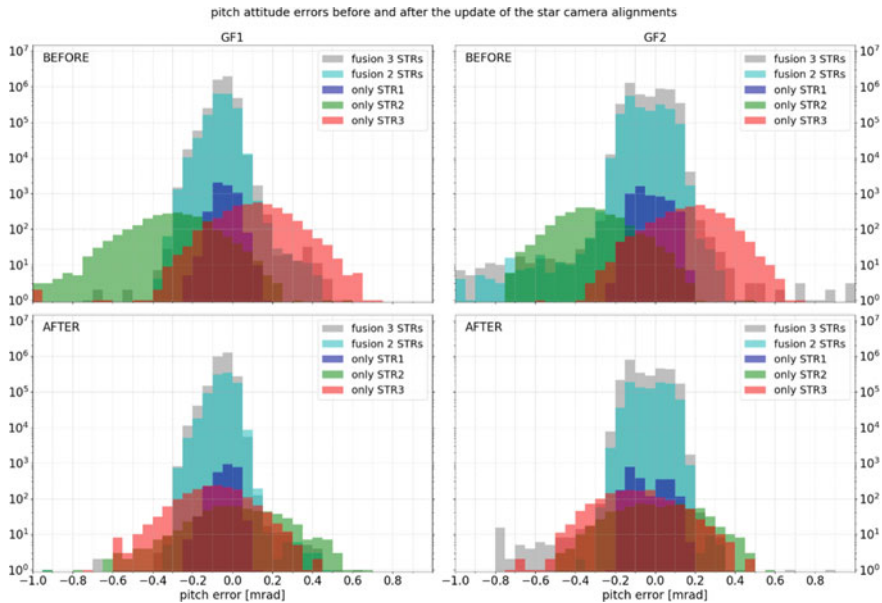


Fig. 4 Distribution of attitude errors along the pitch axis before (top panels) and after (bottom panels) the update of the alignment of the star trackers. On the left side are the attitude errors on GF1 and on the right side the GF2 ones. Due to the considerably smaller size of the data set corresponding to only one star camera head active, a logarithmic scale on the y-axis is used to better display all five data sets at once. Five sets of data are depicted: in grey the attitude error when all STRs are available, in light blue when only two STRs are available and the case when only one star camera is delivering data is displayed in blue, green and red for STR1, STR2 and STR3, respectively

Table 2 Mean and standard deviation of the attitude errors along the pitch axis, as a function of the number of star camera heads used in the fusion process. For each fusion type, values before and after the update of the star trackers alignment are reported

Fusion type		GF1		GF2	
		Before	After	Before	After
3 heads	Mean (mrad)	-0.05	-0.05	-0.03	-0.03
	std (mrad)	0.04	0.04	0.09	0.09
2 heads	Mean (mrad)	-0.04	-0.04	-0.04	-0.02
	std (mrad)	0.05	0.05	0.09	0.08
Only head 1	Mean (mrad)	-0.03	-0.02	-0.04	-0.07
	std (mrad)	0.05	0.04	0.05	0.08
Only head 2	Mean (mrad)	-0.29	0.02	-0.34	-0.05
	std (mrad)	0.17	0.21	0.12	0.18
Only head 3	Mean (mrad)	0.12	-0.10	0.18	-0.09
	std (mrad)	0.15	0.19	0.15	0.17

Table 3 Percentage of days with up to 10, 20, 30 and more than 30 actuations of the pitch thrusters, as a function of the number of star camera heads used in the fusion process. For each fusion type, values before and after the update of the star trackers alignment are reported

Fusion type	Daily actuations	GF1		GF2	
		Before	After	Before	After
2 heads	0–10	100	98	98.6	98
	10–20	0	2	0.34	2
	20–30	0	0	0.34	0
	>30	0	0	0.68	0
Only head 1	0–10	100	100	100	100
	10–20	0	0	0	0
	20–30	0	0	0	0
	>30	0	0	0	0
Only head 2	0–10	40	94	54	97
	10–20	23	3	26	3
	20–30	15	3	8	0
	>30	22	0	12	0
Only head 3	0–10	62	87	66	79
	10–20	20	6.5	10	18
	20–30	8	6.5	9	0
	>30	10	0	15	3

3 Special Activities

3.1 Center of Mass Calibration

Non-gravitational accelerations acting on the spacecraft have to be accurately measured in order to remove their effect on the measurement of the intersatellite distance. Therefore, each GRACE-FO spacecraft carries an accelerometer whose proof-mass is aligned to the center of mass (CoM) of the vehicle. Precise knowledge of the location of the center of mass and the capability of keeping it aligned within 100 μm to the proof-mass is required [2]. The satellite layout was optimized in order to control the offset between the CoM and the ACC proof mass to less than 500 μm in all axes. To keep the CoM offset within the desired range, each satellite is equipped with six movable mass trim mechanisms whose rails are parallel to the three axes of the satellite. Each mass weights ~ 5 kg and can be moved independently in steps of 2.5 μm , allowing for a compensation of the CoM offset up to ± 2.16 mm along the x-axis and ± 1.74 mm along the y- and z-axis.

The propellant tanks are located on the x-axis at the same distance from the CoM. An unequal fuel usage between them and leakages across the thruster branches are expected to induce over time a drift of the center of mass along the x direction.

The center of mass is measured in orbit by means of a center-of-mass calibration maneuver (CMC). A detailed description of its design and of the analysis method to determine the CoM can be found in [9]. A CMC consists of a periodic angular acceleration along the desired axis imposed on the spacecraft using the magnetic torquers. A constant magnetic torque of ± 0.01 Nm is commanded along the selected satellite axis, following a nearly square wave pattern with a pulse width of 5 s and a period of 12 s. Each maneuver consists of 15 of these cycles, for an overall maneuver duration of 180 s. The AOCS executes automatically the maneuver based on the commanded input parameters. Before the calibration starts, the attitude is stabilized by narrowing the dead-bands in all spacecraft axes to 0.5 mrad. These are then set to infinity during the maneuver, resulting in no closed loop attitude control and no usage of attitude thrusters. At the end of a maneuver the closed loop attitude control is resumed automatically. A complete CMC campaign consists of seven maneuvers, two about the roll-axis, two about the yaw-axis and three about the pitch-axis, executed at specific geographic locations.

Two calibration campaigns were executed soon after LEOP. Signature of outgassing in the accelerometer data and an unexpected drift of the center of mass along the x-axis were observed by the science data groups at the Jet Propulsion Laboratory of the Californian Institute of Technology and at the Center for Space Research (CSR) at the University of Texas (Austin). In order to monitor the shift of the center of mass over a complete β' cycle, twelve more campaigns were executed on a monthly basis until October 2019. The offset measured along the x-axis can be compared to the offset expected from the unequal consumption of fuel from the two propellant tanks. The satellite is modelled as five point masses along the x-axis at fixed distance from the CoM [10]. The five bodies are the propellant tanks, the two mass trim mechanisms located along the x-axis and the remaining satellite mass that is fixed and won't change over time. The position of the latter has been estimated by taking as reference a CoM offset measured in orbit. Given the initial outgassing of the satellite, the calibration in February 2019, after the spacecraft went through almost a complete β' cycle and had been illuminated from all sides, has been chosen as reference. The offset of the CoM position calculated from the estimated fuel consumption in the tanks in general represents well the measured one, for both the book-keeping and the PVT methods (see Fig. 5 for GF1). The latter shows some higher fluctuations due to changes of tank pressure and temperature in the different phases of the β' cycle. In February 2020 the trim mass was moved on GF1 in order to maintain the CoM offset within the desired range of ± 100 μ m. The discrepancy observed in the fuel consumption estimated by the PVT and book-keeping methods (see Sect. 2.2.1) is visible also in this analysis. However, the uncertainties associated with both methods have not been evaluated yet and further investigation is ongoing.

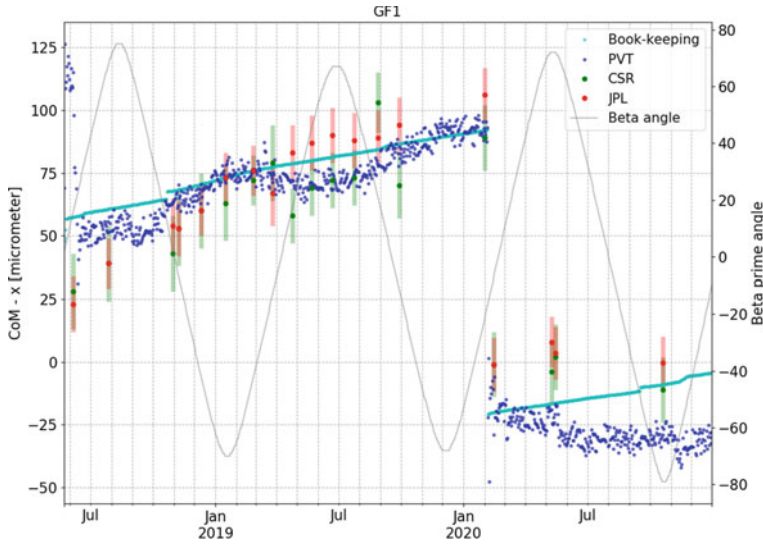


Fig. 5 The offset along the x-axis of the center-of-mass is shown for GF1 over the mission. The CoM offsets measured in orbit during the CMC campaigns are shown in red and green and are based on the estimation from the JPL and CSR science teams, respectively. Superimposed is the estimation of the CoM offset due to the differential consumption of fuel determined with the PVT (dark blue points) and book-keeping (light blue points) methods. The drop in February 2020 is due to a commanded movement of the trim mass to compensate for the accumulate offset. The discrepancy between the PVT and book-keeping methods in the second half of 2020 is currently under investigation. The β' angle is displayed on the right axis

3.2 Fine Tuning of Monitoring and Control Parameters

It was discovered soon after launch that the accelerometers on GRACE-FO display an improper response at short thruster firings, in particular at roll thruster firings [11]. Roll thruster activity is maximum at the geomagnetic equator, where the control authority of the magnetic torquers is drastically reduced in roll. Ways to reduce the overall thruster activity by making less but slightly larger pulses, thereby temporarily accepting larger deviations in roll, were investigated and tested. This was an iterative process that led to a total of three tests, each with a different combination of thruster and NOM-FP controller settings (see Table 4).

The first step was to modify only the settings for the commanding of the roll and yaw thrusters, including the increase of the minimum thruster on-time for the roll and yaw thrusters from 0.05 s to 0.5 and 0.075 s, respectively. The test performed as expected, the number of roll thruster firings was decreased by 85%, but the daily fuel expenditure increased by 50%. The attitude control performance was not affected.

In a second step the number of roll thruster actuations was even reduced by ~97% over a day. The minimum thruster on-time for the roll axis was increased to 1 s and for the yaw axis to 90 ms, and the angular dead bands for the two axes were increased

Table 4 Controller settings in NOM-FP and AOCs performance during each of the tests carried out in order to reduce the number of roll thruster actuations over a day. Tests one to three were performed over 24 h only. The settings of Test 3 were then maintained over a period of three months

	Min Thr ontime (ms)			Angular dead-band (mrad)			Fuel (grams/d)	Daily number of roll thruster actuations
	Roll	Pitch	Yaw	Roll	Pitch	Yaw		
Default	50	50	50	2.5	0.25	0.25	0.7	160
Test 1	500	50	75	2.5	0.25	0.25	1.2	35
Test 2	1000	50	90	5	0.25	0.5	0.94	5
Test 3	1000	100	100	5	0.5	0.55	0.95	8
3-months	1000	100	100	5	0.5	0.55	1.2	14

to 5 mrad for roll and 0.5 mrad for yaw. The fuel consumption was higher than in the nominal configuration, but only by 34%. The extremely low fuel consumption on GRACE-FO provides enough margin to accept this moderate increase. However, also the number of pitch thruster firings increased (from 1 actuation per day, to 35 actuations per day), because of roll/pitch axis coupling through the deviation moment I_{xy} .

Finally, a third set of settings achieved a reduction of the roll thruster actuations by 95%, did not significantly increase the actuations in pitch axis and showed a fuel consumption comparable to what observed in the previous step. The maximum thruster on-time was increased to 1 s for the roll thrusters and to 100 ms for the yaw and pitch ones, and the angular dead bands were enlarged for all axes. Overall no violation of the pointing requirements was observed. This third set of settings was maintained for about 3 months, from November 2018 until February 2019. Over this time the performance could be estimated over a wider range of orbit conditions. The fuel consumption was higher than what observed during the 24 h test period, with on average 1.2 g of cold gas used in a day. It was also observed that with the new configuration a longer stabilization time in the pitch axis was needed when switching between frames of reference. It was decided to permanently revert all settings to defaults on both satellites in February 2019 when the activities to recover GF2 from the OBC switch took place. A method to calibrate the response of the accelerometer to the thruster actuations was investigated.

3.3 Tests to Characterize the Accelerometer Response to Thruster Pulses

A series of thruster tests was executed to model the response of the accelerometers to the actuation of each ACT thruster [12]. Measurements of long pulses were recorded over a range of differential pressures between the two cold gas branches. This could be obtained by spacing out the thrusts by a predefined amount of time.

The backbone of each test is the capability to command the ACTs in open loop. On GRACE-FO it is possible to disable the AOCS control of the thrusters, an FDIR re-enables the on-board control after a configurable amount of time that is by default set to 300 s. During this period the ground operator can command a sequence of thruster activations along the selected axis. The test consists of a sequence of 20 to 60 ACT actuations, each one second long, spaced out by a variable amount of time that ranges between 2 s and 45 min. A different approach is used according to the length of the interval between subsequent thrusts. If the actuations are spaced by less than a minute, they are alternated along the same axis but in opposite directions in order to counteract the attitude deviation created by each single pulse. For sequences requiring some minutes between subsequent firings, the AOCS control on the thrusters is reactivated after each pulse and therefore there is no need to command an alternating sequence. With the thrusters being operated in open-loop, the attitude is controlled only through the MTQs. It is therefore advantageous to execute the tests at geographic locations where the control authority of the magnetic torquer is maximum for the axis along which the ACTs are being fired.

A slight overpressure at the inlet of the attitude thrusters is apparent on branch B on GF1 during nominal operations. The design of the test has therefore to account on GF1 for longer waiting times than on GF2 to allow the pressure to build up to the nominal operational ranges.

On GF1 a total of six tests was executed, with spacings between thrusts of 2 s and of 3, 10, 15, 30 and 45 min. All of them could be executed in NOM-FP over ten days, without interrupting the nominal science data acquisition and with attitude deviations of less than 1.5 mrad in pitch and yaw, and less than 4 mrad in roll. On GF2, a set of six tests was executed with spacings between thrusts of 2 s, 4 s, 7 s, 11 s, 21 s and 15 min. Despite the alternating firing direction and the selection of the optimal geographic location, when commanding thrusts spaced by 4 to 21 s the attitude could drift and attitude errors up to 20 mrad in roll, 4 mrad in yaw and 1.5 mrad in pitch were observed. This part of the tests was therefore executed in the more robust attitude hold mode, resulting however in an interruption of the science mode for about six hours.

The complete set of tests was executed twice, in 2019 and 2020, and the data collected were used by the science data system to calibrate the output of the accelerometer before further using it for the modelling of the gravity field [12].

4 Operations Without Onboard GPS Data

The measurements from the on-board GPS receiver are processed by the IPU yielding a position-velocity-time solution (PVT) at a fixed 2 s interval to the attitude control system. The propagation to the current on-board time is done by a single step, fourth order Runge-Kutta algorithm using a fourth order model of the gravity field. The resulting state-vector is used to generate the so-called reference attitude (see Sect. 2.1). The PVT information is also included in the nominal telemetry stream

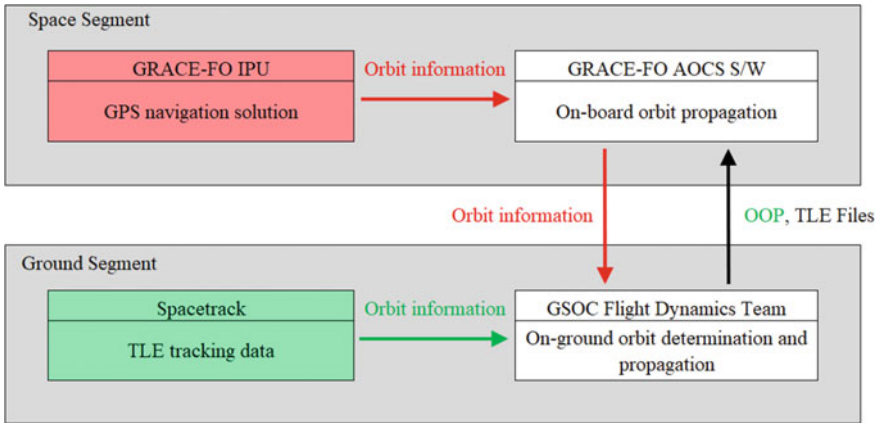


Fig. 6 A simplified diagram for the flow of position and velocity information between space- and ground-segment. The source will be changed to data from SpaceTrack (green box) in case of a prolonged unavailability of the IPU or of the on-board GPS receiver

and used for precise orbit determination from long data arcs. The result for the two satellites is then up-linked at least once per day to both in the form of Two-Line-Elements (TLE). The continuous knowledge of the own and of the other’s position enables the accurate pointing required in the science mode (see Sect. 2.1).

The last valid measurement will be used and propagated if for some reason no data from the GPS receiver are available (could be caused by either a receiver, or an IPU outage). The accuracy for the required relative pointing deteriorates rather quickly and an on-board FDIR will trigger a transition into safe mode if the outage persists for more than 24 h. Longer receiver or IPU outages (e.g., due to planned maintenance or a switch-over) can only be bridged in NOM if the on-board orbit propagator (OOP) is updated regularly with fresh information from ground. The uplinked state vector will then no longer be based upon the satellite’s own GPS measurements, but is computed from orbit data provided by SpaceTrack¹ (see Fig. 6). This decreases the overall pointing accuracy somewhat due to the lower frequency and quality of the delivered orbit data, and the precision of the on-ground orbit determination and propagation.

In 2018 the prime IPU on GF2 was powered down by an FDIR. A prolonged period of tests was finally followed by the decision to switch to the redundant side. This took several months in total because the complete instrument chain (including not only the IPU, but also the instrument control unit and the microwave tracking system) had to be switched. Orbit determination was based upon SpaceTrack data during this time and OOP updates were sent to GF2 every 2nd, or 3rd day only. No attempt was made to maintain the science configuration as discontinuities of up to 4 mrad in pitch were observed at each update.

¹ <https://www.space-track.org/>.

This prompted an investigation to see whether a method could be developed to cope with long GPS data outages and still maintain sufficient accuracy to uphold relative pointing and to continue science. An analysis of such a method and of the effects on the inter-satellite pointing is investigated in the following two sections. It will be shown that science can be continued even in the worst-case scenario of a permanent unavailability of on-board GPS data on one of the satellites.

4.1 Improvement When Using Data from SpaceTrack

Standard available TLEs from SpaceTrack had to be used to feed the OOP for GF2 between 2018-07-19 and 2018-10-16, due to unavailability of GPS data. Previous experience shows that a single TLE can be rather imprecise, leading to an apparent discontinuity in the relative position between GF2 and GF1 when the OOP is re-initialized based on such input. This in turn brings about a physical reaction of the attitude control system and might lead to the loss of the inter-satellite link (see Sect. 4.3 for a discussion on the allowed tolerances). Therefore a modified approach, applying a fitting algorithm over several TLE's, was developed.

Two sets of TLEs are normally provided by SpaceTrack each day for each of the GRACE-FO satellites. Taking all TLEs of the last 5 to 7 days and using a SGP4 propagator [13] ephemerides between each of the TLEs' epochs were created. These were then concatenated and handled as standard GPS data, i.e. an orbit determination (OD) over the complete period was made. The OD comprises a batch least-squares fitting algorithm, which allows the determination of a smoother orbit by excluding data from a rather imprecise single TLE. In this way the mentioned discontinuities from one TLE to the next one are strongly reduced.

The method was analysed for a period of three months between July and October 2019 by comparison with the nominal OD that is based upon the on-board GPS data. The results of both types of orbit determinations (state-vectors at a given epoch) were then propagated over ~ 24 h² and the position offsets compared over one orbit. The statistics over 103 days are presented in Table 5 using the RTN-frame (radial-tangential-normal³). The largest offset found were 150/4300/160 m in RTN-frame.

The above method requires periods without orbit maneuvers. A different approach would have to be developed for satellite missions with frequent orbit changes, e.g., maneuvers on a daily basis. Also, the analysis was performed over a 100-day period only and during a minimum in the solar cycle. The offsets as shown in Table 5 might differ considerably at other phases in the 11-year solar cycle due to increased solar radiation pressure and atmospheric drag.

² The OD results are used to provide on-board orbit products for the next 24 h. The accuracy of these products should be of sufficient quality, which is why an analysis period of 24 h was realized.

³ Its origin is at the satellite position; the x-axis is aligned with the radial vector that points from the center of the Earth to the satellite (positive outwards), the z-axis is aligned to the normal direction

Table 5 Comparison between orbit determinations based upon on-board GPS data (reference) and from an algorithm fitting up to 14 TLE’s (see text). The offsets in the RTN-frame are computed over one orbit after a propagation over a period of 24 h

	R (m)	T (m)	N (m)
Minimum	-150	-3600	-150
Maximum	130	4300	150
Mean	0	10	0
1-Sigma	70	1500	60

4.2 Accuracy of the On-Board Orbit Propagation

An analysis of the overall errors associated with the approach as described in Sect. 4.1 was made over a period of three days that had ODs based upon on-board GPS data, as well as from the algorithm using SpaceTrack TLEs available. The results are shown in Fig. 7. A fresh state vector with epoch 17:00 UTC was ingested by the OOP each day. The results of the OOP are then compared with the directly measured GPS position and velocity on-board. It is seen that the position error in tangential direction is significantly larger than in radial, or normal direction. The deviation in velocity, however, is largest in radial direction. The discontinuity after each upload

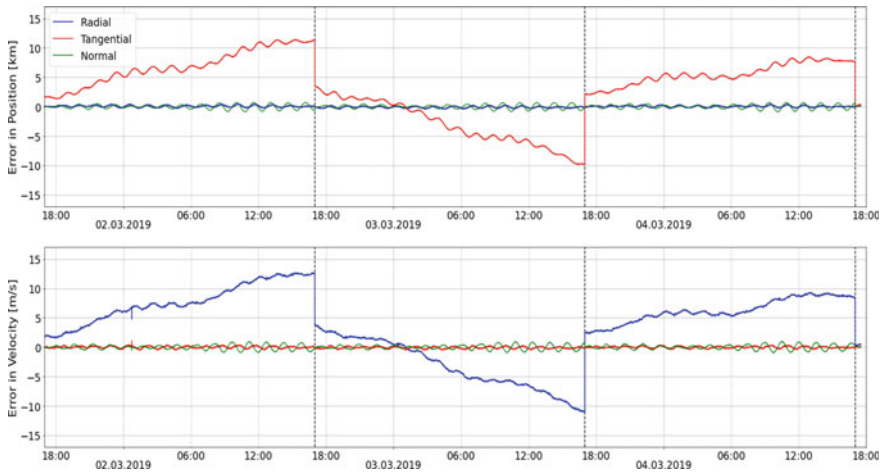


Fig. 7 Position and velocity errors in the RTN-frame are shown over a period of three days. These are computed from a comparison of the on-board GPS measurements with the results of the on-board orbit propagation (OOP). The OOP was re-initialized each day at 17:00 UTC by up-linking the result of an orbit determination (OD) based upon several days of SpaceTrack data. The error in position is dominated by its tangential, in velocity by its radial component

perpendicular to the radial and velocity vector, and the y-axis completes the right-handed system pointing in the tangential direction.

Table 6 The deviation in the RTN-frame of the OOP with respect to the on-board GPS measurements is shown as a function of the upload frequency. Data have been averaged over a three day period

	OOP update frequency	R (km)	T (km)	N (km)
Maximum error	Every two days	0.5	21.0	-0.1
	Once per day	0.5	11.4	0.9
	Twice per day	-0.4	7.0	-0.6
Maximum jump during update	Every two days	<0.1	18.7	<0.1
	Once per day	0.2	12.1	0.7
	Twice per day	0.2	8.1	0.3

is due to the uncertainty in the method of fitting the SpaceTrack TLEs. The small periodic variations that are visible, are related to the position in orbit.

The maximum deviation of the OOP and the magnitude of the jump at upload are of direct interest for science, i.e. for keeping relative pointing within the prescribed limits. These numbers (averaged over three days period) can be found in Table 6 for three different update frequencies. It can be seen that the maximum position error is ~7 km in tangential direction for an update frequency of twice per day (maximum for GRACE FO in the routine phase). Deviations increase to approximately 11 km and 21 km if the uplink frequency goes down to once per day, or once per two days, respectively (e.g., due to problems at the ground station). The maximum jump occurs at the moment that the OOP is re-initialised and its size comparable with the maximum deviations found.

4.3 Analysis of the Guidance Angles

The science mode requires that the front-ends of the satellites point towards each other (relative pointing—see Sect. 2.1.2 for a detailed description). The guidance angles are defined as the difference between the Relative Pointing Frame and the Nadir Pointing Frame and are calculated on-board from a propagation of the uplinked TLEs (also for the other satellite). A rough indication of these three angles is $(0, -1^\circ, 180^\circ)$ for the leader and $(0, -1^\circ, 0^\circ)$ for the follower, but exact guidance depends upon inter-satellite distance, eccentricity, inclination and also upon the quality of the TLE's and their upload frequency. The acceptable errors are dictated by the Laser Ranging Instrument (LRI). A pointing accuracy of ~300 μ rad is required for first acquisition, but errors of up to 5 mrad are possible before lock is lost once the link has been established.

The guidance angles in pitch and yaw, and their respective errors, are shown over a period of 5 days when no on-board GPS data were available on one of the satellites (see Fig. 8). The upper two panels show the situation when the OOP was updated twice per day. It can be seen that the errors remain well within the 5 mrad boundary

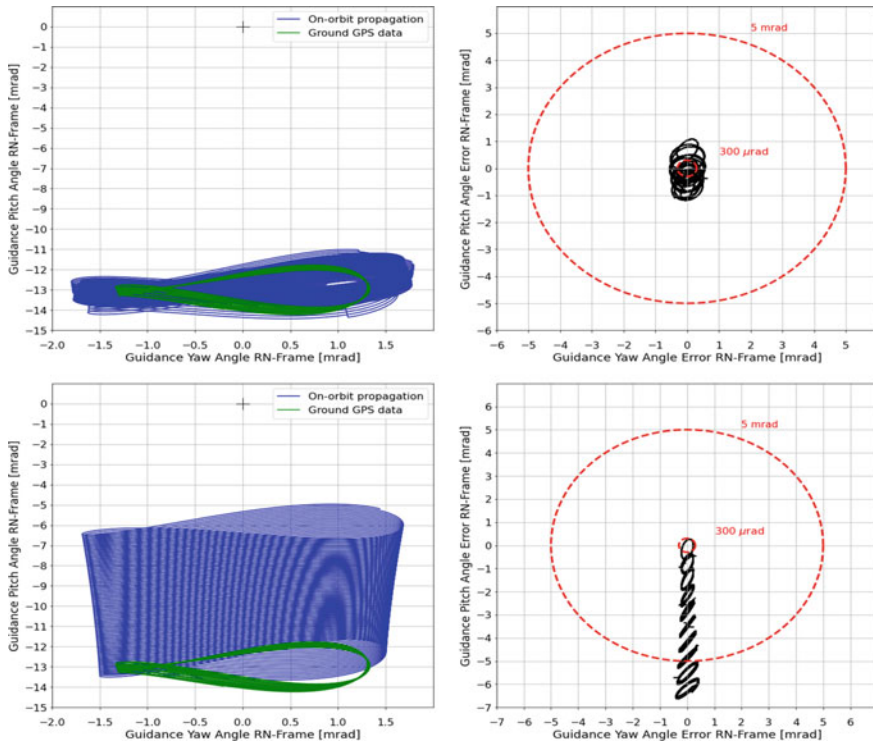


Fig. 8 The guidance angles in pitch and yaw and their errors are shown over a period of 5 days with on-board GPS data missing on one of the satellites. The computation is based upon the OOP, which is re-initialised twice per day in the upper two panels and not at all in the lower two. The RN frame describes the attitude differences between the relative pointing- and nadir- pointing frames. Only a few orbits are shown for clarity

after which LRI lock will be lost. An appreciable part of the time the errors are $<300 \mu\text{rad}$, implying that the link can be re-established. This is compared in the lower two panels with the case when the OOP is not updated at all. Already after one day a re-acquisition is no longer possible and the limit of 5 mrad is violated after three days. Note that the roll-angle is not very important for the pointing of the LRI and therefore not shown. Also note that the errors in pitch angle are much larger than the ones in yaw. The reason is the larger deviation in position found for the tangential direction (see Fig. 7).

The observed angle deviations are mainly due to the simplified gravitational model of the on-board propagator, together with the fact that the effect of the aerodynamic drag is not included. An overview of the maximum error, as well as the maximum jump, in pitch and yaw during the upload of OOP and TLE data is shown in Table 7.

This analysis, although preliminary because only a short interval near solar minimum could be included, shows that it is possible to continue full science operations even when no on-board GPS data are available on one of the satellites. A next

Table 7 The maximum error and jump in the pitch and yaw guidance angles are shown as a function of the frequency of OOP and TLE update

	OOP/TLE update frequency	Pitch (mrad)	Yaw (mrad)
Maximum error	Every two days	3.2	0.5
	Once per day	2.0	0.6
	Twice per day	1.2	0.6
Maximum jump during update	Every two days	2.7	0.2
	Once per day	1.8	0.1
	Twice per day	1.2	0.1

step could be to investigate the influence of different aerodynamic drag. Also, long-term simulations, including the variation of the angle between the orbital plane and Sun-direction, must be made to demonstrate the feasibility of the described approach. The ability of the instruments to fulfil their performance requirements under these conditions must also be assessed.

5 Conclusions

The performance of the AOCS of the GRACE Follow-on satellites was stable over their first years in orbit, benefiting also from the lessons learned from the GRACE mission. With a remarkably low fuel consumption, the life expectancy based solely on the expenditure of this resource is a factor of ten higher than the initially planned mission duration of five years. A minor difference between the two tanks of the cold gas system has been observed on both satellites, but the uncertainties associated with the methods to estimate the remaining cold gas mass still have to be fully investigated.

The settings for attitude control in normal mode were varied and several thruster tests carried out to help the science team to calibrate the measurements of the accelerometer.

A method to bridge long phases without a functional GPS receiver has been developed and was used on one of the satellites for the several months in which the switch to the redundant instrument chain was prepared. During this time, however, the science data acquisition was interrupted. A preliminary analysis showed that the pointing accuracy will be sufficient to support instrument operations in the worst-case scenario of the loss of the redundant chain. Further tests to improve on the performance will be needed in that case.

Acknowledgements The Gravity Recovery and Climate Experiment Follow-on (GRACE-FO) mission is a partnership between NASA and the German Research Centre for Geosciences (GFZ). Mission Operations for the first 5 years are funded by GFZ and sub-contracted to DLR's German Space Operation Center (GSOC) in Oberpfaffenhofen.

The authors would like to thank the Science Data System teams at JPL and CSR for their help and fruitful discussions during the first years of life of the GRACE Follow-on satellites.

References

1. Tapley BD, Bettadpur S, Watkins M, Reigber C (2004) The gravity recovery and climate experiment: mission overview and early results. *Geophys Res Lett* 31, Paper L09607
2. Kornfeld RP, Arnold BW, Gross MA, Dahya NT, Klipstein WM, Gath PF, Bettadpur S (2019) GRACE-FO: the gravity recovery and climate experiment follow-on mission. *J Spacecr Rocket* 56:931–951
3. Landerer FW, Flechtner FM, Save H, Webb FH, Bandikova T, Bertiger WI et al (2020) Extending the global mass change data record: GRACE follow-on instrument and science data performance. *Geophys Res Lett* 47:e2020GL088306
4. Abich K, Abramovici A, Amparan B, Baatzsch A, Bachman Okihiro B, Barr DC et al (2019) In-orbit performance of the GRACE follow-on laser ranging interferometer. *Phys Rev Lett* 123:031101
5. Witkowski MM, Gaston R, Shirbacheh M (2021) GRACE follow-on early in-flight challenges. In: 16th international conference on space operations, Cape Town, South Africa, 3–5 May
6. Löw S, Cossavella F, Herman J, Müller K, Davis E, Save H (2019) Attitude and orbit control of the grace satellites at extremely low power. In: IAC-19-B.6.3.2, 70th international astronomical congress (IAC), Washington D.C., United States, 2019, 21–25 October
7. Herman J, Presti D, Codazzi A, Belle C (2004) Attitude control for GRACE. In: ESA SP-548: 18th international symposium on space flight dynamics, Munich, Germany
8. Wirth K, Löw S, Müller K, Snopek K, Gaston R (2021) The challenge and consequences on mission operations after inverting a complex failure management concept in-orbit. In: SpaceOps-2021,3,x1438, 16th international conference on space operations, Cape Town, South Africa, 2021, 3–5 May
9. Wang F, Bettadpur S, Save H, Kruizinga G (2010) Determination of center-of-mass of gravity recovery and climate experiment satellites. *J Spacecr Rocket* 47:371–379
10. Lex F (2015) Analyse von Anomalien innerhalb des Kaltgas-Systems der low-earth-orbit satellite mission GRACE. Diploma Thesis, Hochschule München
11. McCullough CM, Harvey N, Save H, Landerer FW, Webb F (2019) Accelerometer modeling and calibrations for GRACE-FO. In: AGU fall meeting abstracts, G51B0590M
12. McCullough C, Harvey N, Save H, Bandikova T (2019) Description of calibrated GRACE-FO accelerometer data products (ACT). In: JPL D-103863, NASA Jet Propulsion Laboratory, California Institute of Technology
13. Hoots Felix R, Roehrich Ronald L (1980) Models for propagation of NORAD element sets: Spacetrack rept. no. 3, Aerospace Defense Command, United States Air Force